



Symmetry Violations and Rare Decays*

R. Coleman², B. Winstein⁸, G. Bock², M. Cooper⁴, J. Enagonio², A. Erwin¹⁰, J. Fry⁹,
H. Greenlee¹¹, B. Hsiung², K. McFarlane⁷, W. Morse¹, T. Shinkawa³, G. Thomson⁶,
B. Tschirhart⁵, Y. Wah⁸, H. Yamamoto⁸, T. Yamanaka²

¹Brookhaven National Laboratory, Upton, New York 11973

²Fermi National Accelerator Laboratory, P. O. Box 500, Batavia, Illinois 60510

³National Laboratory for High Energy Physics (KEK), Ibaraki 305, Tsukuba, Japan

⁴Los Alamos National Laboratory, Los Alamos, New Mexico 87544

⁵Princeton University, Princeton, New Jersey 08540

⁶Rutgers University, Piscataway, New Jersey 08854

⁷Temple University, Philadelphia, Pennsylvania 19122

⁸University of Chicago, Chicago, Illinois 60637

⁹University of Liverpool, Liverpool L69 3BX, England

¹⁰University of Wisconsin, Madison, Wisconsin 53706

¹¹Yale University, New Haven, Connecticut 06520

December 1989



* Summary report from "Physics at Fermilab in the 1990's," Breckenridge, Colorado, August 15-24, 1989.

Symmetry Violations and Rare Decays

R. Coleman², B. Winstein⁸, G. Bock², M. Cooper⁴, J. Enagonio², A. Erwin¹⁰, J. Fry⁹, H. Greenlee¹¹, B. Hsiung², K. McFarlane⁷, W. Morse¹, T. Shinkawa³, G. Thomson⁶, B. Tschirhart⁵, Y. Wah⁸, H. Yamamoto⁸, T. Yamanaka²

¹Brookhaven National Laboratory, ²Fermi National Accelerator Laboratory, ³KEK National Laboratory, ⁴Los Alamos National Laboratory, ⁵Princeton University, ⁶Rutgers University, ⁷Temple University, ⁸University of Chicago, ⁹University of Liverpool, ¹⁰University of Wisconsin, ¹¹Yale University

ABSTRACT

This constitutes the report of the working group on symmetry violations and rare decays. The next generation of CP violating kaon decay experiments (the 2π and $\pi^0 e^+ e^-$ modes) were considered at the Tevatron and at the proposed Main Injector, effectively building upon the work of the earlier Fermilab Workshop on Physics at the Main Injector. The optimizations for the electromagnetic calorimeter and for background rejection are treated in some detail. Very precise CPT tests in the 2π decay modes are also treated. A sensitive experiment looking for flavor violation at the Main Injector ($K_L \rightarrow \mu e$) is discussed. The significant advantages of possible stretcher and prebooster rings are mentioned.

1. INTRODUCTION

This group considered a variety of physics issues which are accessible with very intense kaon beams. Beams at the Tevatron were considered, along with new beams at the proposed Main Injector which offer substantially increased opportunities. We first treat the next generation of experiments of CP and CPT symmetry tests with the two-pion decays of the neutral kaon. Next we discuss in some detail possibilities for observing direct CP violation in other modes, notably in $K_L \rightarrow \pi^0 e^+ e^-$. After a brief discussion of a $K_L \rightarrow \mu e$ search, we close with a mention of possible future upgrades.

2. NEW MEASUREMENTS OF ϵ'/ϵ AND CPT TESTS

2.1. The 2π Decay Modes: ϵ'/ϵ Determination

As is well known, the determination of ϵ'/ϵ is accomplished with precision measurements of the following four decay modes:

$$K_S \rightarrow \pi^0 \pi^0, \tag{1}$$

$$K_L \rightarrow \pi^0 \pi^0, \tag{2}$$

$$K_S \rightarrow \pi^+ \pi^-, \tag{3}$$

$$K_L \rightarrow \pi^+ \pi^-, \tag{4}$$

Then, by forming the double ratio:

$$R = (1)/(2)/[(3)/(4)] = 1 + 6 \operatorname{Re}(\epsilon'/\epsilon) \tag{5}$$

one can extract the value of ϵ'/ϵ .

The situation regarding current measurements of this quantity is shown in the following Table (in units of 10^{-4}):

Table 1. Recent Measurements of $\text{Re}(\epsilon'/\epsilon)$

Experiment	Result	Statistical Error	Systematic Error	Combined Error
BNL-YALE	+17	72	43	83
Chicago-Saclay	-46	53	24	58
E731 Test	+32	28	12	30
NA31	+33	7	8	11
E731	-5	14	6	15

where the last entry is the latest (preliminary) result from a 20% analysis of the Fermilab E731 data set. It is seen that E731 does not confirm the CERN NA31 experiment which claimed significant evidence of direct CP violation for the first time.

How might this situation evolve? Clearly motivation for an improved experiment must wait on the full analysis of the E731 data set: the discrepancy with NA31 is at the 2σ level now, but if the E731 result remains consistent with zero with the full data set, then the Superweak hypothesis will be very much viable and the Standard Model will remain unconfirmed.

We first consider what could be done further at the Tevatron, based upon the E731 experience.

An upgrade to E731 could certainly collect the statistics for a much improved determination. However, the crucial factor will be systematic uncertainty. In the following Table, we list the major sources of uncertainty and an estimate of the possible improvements attainable at the Tevatron.

Table 2. Systematic Uncertainties [%] in the Double Ratio R

Effect	E731	E731 Upgrade	Main Injector
Charged Background	0.06	0.01	0.01
Neutral Background	0.07	0.04	0.01
Neutral Non-linearity	0.20	0.10	0.01
Acceptance	0.25	0.08	-
Regenerator Scattering	0.16	0.05	0.01
Systematic Total	0.37	0.14	0.02
Statistical Error	0.84	0.12	0.03
ϵ'/ϵ Statistical Error [10^{-4}]	14 \rightarrow 5	2	0.5
ϵ'/ϵ Systematic Error [10^{-4}]	6 \rightarrow 4	2	0.3

The presently reported sample of E731 data has a statistical (systematic) accuracy of 14 (6) in units of 10^{-4} . With the data in hand, these should be reduced to 5 (4). We will comment on the various table entries relevant towards a future Tevatron Upgrade.

Charged Background. The background in the charged mode is largely the semileptonic $\pi e \nu K_L$ decay. The associated systematic uncertainty can be reduced by a factor of 6 by further rejecting this background. This will be accomplished with the transition radiation detectors (TRDs) which are being constructed for Fermilab E799.

Neutral Background. The neutral background results from mis-reconstructed $3\pi^0$ decays which fake $2\pi^0$ ones. The uncertainty associated with this background can be somewhat reduced with the addition of a finer celled calorimeter (as will be done for E791) in the central region of the detector: the major background arises from so-called "fusion events" where two photons are too close in the lead-glass array to resolve.

Neutral Non-linearity. This systematic uncertainty results from an incomplete understanding of the response of the lead-glass, in particular of its energy dependence. With the replacement of the glass with BaF_2 in the central region, this uncertainty will be reduced; BaF_2 is more linear. Additionally, it is thought that this uncertainty can be reduced with more study of the present data.

Acceptance. The estimated acceptance uncertainties for E731 are conservative and in fact they can probably be reduced significantly with a little more work. It is estimated that in a new Tevatron experiment, this systematic uncertainty will come down by a factor of about 3.

Regenerator Scattering. In E731, K_S and K_L decays to $2\pi^0$ are simultaneously collected by means of a double K_L beam in one of which a regenerator is placed. The two decays are distinguished with the "center-of-energy" in the calorimeter. However, there is a significant amount of scattering from the regenerator so that events which originate in that beam can be found in the vacuum beam. In principal, this effect can be determined from the distribution of the scattered events in the charged mode (where the scattering angle is measured), but a small residual uncertainty remains. This can be reduced with the use of a totally active regenerator (made of scintillator) which will be employed for Fermilab E773.

Statistical Precision. The achievement of a statistical precision of 2×10^{-4} in ϵ'/ϵ will require the collection of about 2×10^6 $K_L \rightarrow 2\pi^0$ decays or about 6 times that collected in E731. This is achievable with a slight increase in intensity and with more sophisticated trigger processors. Such a processor for charged decays will be

employed in 1973 and very likely one for neutral decays will be used for the second phase of E799.

Such a Tevatron experiment could probably be performed in the 1992/1993 period; it would have a precision of about 3×10^{-4} (perhaps even better) and as such would be able to "establish" direct CP violation if ϵ'/ϵ is larger than 0.001 as is likely in the Standard Model. If even this experiment produces a null result, then to make additional progress we must go to a much more intense kaon beam. Here we consider that which would be provided by the proposed new Main Injector for Fermilab. The possibilities in this direction have been treated in Ref. 1. There is the capability of achieving a branching ratio sensitivity on the order of 10^{-10} per hour of running, using the full proton flux and a beam of about $36 \mu\text{str}$. Such a configuration will be necessary for the studies of rare decays with sensitivities in the range of 10^{-13} ; however for the following generation experiment measuring ϵ'/ϵ , considerably less flux is required and so smaller beams can be employed.

2.2. ϵ'/ϵ at the Main Injector

2.2.1. Technique and statistics. We set as our goal the improvement of another factor of about 5 over the upgraded Tevatron experiment, namely to reach a statistical precision of 5×10^{-5} with a substantially smaller systematic uncertainty. We consider the following variation on the double beam technique of E731. With a thin regenerator in a pure K_L beam, the outgoing amplitude will be given by $K_L + \rho K_S$ where ρ is the regeneration amplitude. We choose $\rho = 1.5\eta$ so that, in the first 3 lifetimes downstream of the regenerator (region A) the 2π decay rate is dominated by K_S decays while in the next three lifetimes (region B) K_L decays dominate. Then, by measuring decays from both modes ($\pi^+\pi^-$ and $2\pi^0$) and in both regions, the double ratio (5) can be formed and ϵ'/ϵ extracted. The uncertainty due to regenerator scattering can be greatly reduced (see Table 2) with the smaller beams and thinner

regenerator. A much more linear calorimeter is required and it appears that BaF_2 will have the required characteristics as will be discussed later. In Figures 1 and 2 are shown a possible layout of the beam line and detector and of the electromagnetic calorimeter.

It may be possible to determine the acceptance variation for both modes by means of Monte Carlo. However, by measuring decays at analogous lifetimes (Region C and Region D) in a nearly parallel identical beam, the acceptance can be directly determined thereby eliminating this as a source of uncertainty. The flux at the Main Injector allows this technique to work. In the following Table, we give the fluxes and decay rates for this configuration.

Table 3. Fluxes and Rates for an ϵ'/ϵ Experiment at the Main Injector

Proton Flux	3×10^{13} per spill
Kaon Flux	16 MHz
Neutron Flux	14 MHz
Kaon decays [20 m decay region]	0.9 MHz

Accepted $K_L \rightarrow 2\pi^0/\text{hour}$

Region A	40K
Region B	13K
Region C	13K
Region D	13K
Precision/hour	1.6%
Hours/0.03% precision	2800

We note that this configuration uses the anticipated full flux of the Main Injector but that the kaon intensity is not at its maximum because of the small beam size. The intensity in the beam will allow the insertion of the thin regenerator without too much load on the apparatus.

The mean accepted kaon momentum will be about 20 GeV so that the three lifetime region will correspond to approximately a 3 m region. For this configuration, the acceptance is about 30% for

the $2\pi^0$ decay mode and the entire statistics of E731 could be obtained in a one day run.

2.2.2. Trigger and data acquisition. Assuming two 1" x 1" kaon beams, one expects ~ 1 MHz of kaon decays in a 20 m decay volume. We would then expect a (deadtimeless) yield of ~ 75 Hz "good" $\pi^0\pi^0$ decays and ~ 400 Hz "good" $\pi^+\pi^-$ decays from K_L and K_S together with kaon momentum between 15 to 50 GeV in a 8 m decay volume. This is almost a 100 fold increase in yield compared with E731.

The expected raw trigger rate using the current E731 trigger would give ~ 100 kHz for the $\pi^0\pi^0$ mode (requiring 4 distinct photon clusters and a 10 GeV total energy threshold in the electromagnetic calorimeter) and ~ 700 kHz for $\pi^+\pi^-$ mode (requiring two non-muon tracks in the hodoscope banks and wire chambers). Further trigger reductions are crucial to give a reasonable event rate to "tape". On-line processors (such as a cluster finder and track finder), electron rejection from TRDs and E/p cut based on the matched track and electromagnetic cluster, etc., will be needed to cut the trigger rate down by a factor of a few hundred. We anticipate reaching a trigger rate of 500 (1500) Hz for the $\pi^0\pi^0$ ($\pi^+\pi^-$) mode. This is possible, but quite challenging.

The proposed final event rate is ≥ 2 kHz to "tape". Assuming 1.5 kByte per event, it will require writing more than 3 MByte/s onto either high density "tape" or "disk". Therefore, an advanced data acquisition system and fast, large data storage devices and drivers are required to handle the expected high data rate.

2.2.3. Electromagnetic calorimeter. Future kaon experiments at high intensities place a set of stringent requirements on electromagnetic calorimeters:

Fast timing. The expected high rate will result in accidental overlaps that limit sensitivities of some rare kaon decays and contribute to systematics in precision measurements such as the

measurement of ϵ'/ϵ . Both the pulse width and the time resolution of the leading edge must be small (a few 10's of ns for the former and 1 ns or less for the latter).

Radiation hardness. The calorimeter should withstand radiation levels of order 10^4 rad without appreciable degradation of performance.

Good resolution. In some rare decays, good resolution is essential in effective background rejection; also, the calibration of energy scale to less than 0.1% (e.g. for the measurement of ϵ'/ϵ) requires that the energy resolution be a few % or less for typical electromagnetic showers.

High density. Two nearby showers that cannot be separated can become a major source of background in such decay modes as $2\pi^0$ and $\pi^0\gamma\gamma$. Thus the transverse size of the shower (namely the Moliere radius of the material) must be small (a few cm or less).

Stability. The response should not have strong dependences on temperature and rate.

The timing requirement excludes BGO (decay time 300 ns) and CsI(Tl) (decay time 1 μ s). Also, these crystals do not pass the requirements for radiation hardness. Scintillating glasses tend to have respectable resolutions; their radiation length, however, is typically 4 cm and the transverse shower size is accordingly large. Gas sampling type calorimeters are not suitable due to their poor resolutions. Thus, we have selected pure CsI, BaF₂, PbF₂, and lead-scintillating fiber as candidates to be studied.

CsI(pure). The scintillation has fast components (10ns and 30ns) and a slow component (a few μ s)²⁾. The fast emission is at 305 nm and phototubes with UV glass windows can be used instead of more expensive ones with quartz windows. The slow component is quite sensitive to heat and mechanical shock as well as to impurities. The fast component is more stable; the temperature dependence of the light output, however, is quite large (1.5%/degree)³⁾. The radiation hardness is on the borderline

of being acceptable³), but the fast component may not be fast enough in a high-rate environment.

BaF₂. The emission spectrum has fast components at 195 nm and 220 nm with a decay time of 0.6 ns and a slow component at 300 nm with a decay time of 600 ns⁴). The light output of the slow component is 5 to 10 times larger than the fast component; thus, it has to be suppressed in order to operate at a high counting rate. Several methods have been tried:

a) Coupling with TMAE⁵). It is difficult to cover a large area without dead regions with this scheme.

b) Solar-blind phototube⁶). A Cs-Te photocathode has its sensitivity only in the UV region. The slow component is reduced by about factor of 7, which is probably enough for our case.

c) La³⁺ doping⁷). This method is quite new and the technique to make long crystals with uniform doping has not been perfected at present.

d) UV bandpass filter. The transmission at peak is typically 30%, and FWHM is about 40 nm. When light yield is not a problem, this could be a viable option (e.g. combined with a solar-blind phototube.).

The crystal is quite expensive and the short wave length of the fast component requires phototubes with quartz windows. BaF₂ is, however, remarkably resistant against radiation (up to 10⁷ rad)⁸).

PbF₂. This material has been recently rediscovered as a promising Cerenkov radiator⁹). It is very dense (7.7 g/cm³) and accordingly the radiation length is short (0.95 cm). The Moliere radius is 2.2 cm, but the apparent transverse shower size is even shorter by about 25% since the Cerenkov light is emitted less in the tails of the shower with respect to dE/dx energy deposition. The technique to manufacture pure and transparent crystals has not been established yet but seems to be a matter of commitment rather than of technical difficulties. Compared with lead-glass (F-2 with filter), the light output of PbF₂ is about 3 times larger. This is

partly due to the wider bandwidth and to the fact that it does not require any filter, since the cutoff of borosilicate window of phototube is expected to provide the equivalent function. Thus, if the transparency of PbF_2 crystal can be made 1% per radiation length or less, then energy resolution of $3\%/\sqrt{E}$ seems attainable. The radiation hardness of the material is not established, but with less pure samples, the results seem promising⁹⁾.

Lead-scintillating fiber. Recently, energy resolutions of $6\%/\sqrt{E}$ have been reported for a lead block with scintillating fibers embedded¹⁰⁾. The module is inexpensive ($\sim \$0.4/\text{cm}^2 X_0$), and can be fabricated into various shapes. The response, however, strongly depends on the incident angle of particles (especially photons) with respect to the fiber direction. Also, the resolution reported is not adequate even though it is quite respectable. We have simulated a module using EGS4 to see if the geometry can be further optimized for better resolutions. Figure 3 shows the result: the larger the fiber fraction by volume and the smaller the fiber diameter, the better the resolution becomes. Also, the honeycomb geometry gives about 6% better resolution than square geometry for a given fiber radius and fiber fraction by volume. The best reasonably obtainable resolution is about $5\%/\sqrt{E}$ which still is not good enough as a main calorimeter for the next generation of kaon experiments. The low cost and geometrical flexibility, however, make it a good candidate for photon vetoes.

The properties of the candidates are summarized in Table 4; lead-glass (F-2) is also included for comparison. It seems that PbF_2 and BaF_2 are the most desirable candidates, while CsI (pure) could be viable if the temperature dependence can be controlled and the rate is not very high (accidental pile-up effect and radiation damage).

Table 4.
Comparison of Electromagnetic Calorimeters

	Pb-Glass F-2 w/filter	PbF ₂	BaF ₂ w/Cs-Te PMT	CsI w/quartz PMT	Pb-SciFi 60% fiber 1mm ϕ
X ₀ radiation length(cm.)	3.13	0.98	2.1	1.85	1.47
Moliere radius (cm.)	4.5	1.8	3.5	4.4	5.0
index of refraction	1.64	1.86	1.56	1.86	- -
decay time	Cerenkov	Cerenkov	0.6 ns + slow	10ns,30ns and slow	< 10ns
#p.e./MeV	0.5	1.5	> 30	>100	1 ~ 2
ultimate $\sigma/\sqrt{E}(\%)$	5	3	1	0.7	5
attenuation per X ₀ (%)	3	~ 1(?)	< 1	~ 1	~ 1
radiation damage @ (rad)	10 ⁴	> 10 ⁶	10 ⁷	10 ⁴ ~ 10 ⁵	10 ⁵ ~ 10 ⁶
Price \$/cm ² X ₀	1	2	12	5	0.4

2.3. The 2π Decay Modes: CPT Test

The K^0 system gives the possibility of separately measuring CP, T and CPT violating amplitudes. Very high statistical precision is required, together with tight control of systematic errors. With current detector technology this is only possible with separated beams of K_L and either regenerated or target K_S . The measurable parameters, and their relationship to the theoretical amplitudes, are discussed below. A brief discussion is given of a possible experiment to achieve the desired precision.

In the decay of a neutral kaon to two pions all of the physics is embodied in the two complex parameters η_{+-} and η_{00} , the ratio of the decay amplitudes for a K_L and K_S to $\pi^+\pi^-$ and $\pi^0\pi^0$. These parameters are related to the CP, T and CPT violating amplitudes as follows:

$$\eta_{+-} = (\epsilon - \delta) + (a + \epsilon') / [(1 + \omega)(1 + a(\epsilon + \delta))] \quad (6)$$

$$\eta_{00} = (\epsilon - \delta) + (a - 2\epsilon') / [(1 - 2\omega)(1 + a(\epsilon + \delta))] \quad (7)$$

where

- ϵ and δ are T and CPT violating amplitudes, respectively, in the mass matrix ($|\Delta S| = 2$).
- a is a CP and CPT violating (T conserving) term in the $I = 0$ decay amplitude ($|\Delta S| = 1$).
- ϵ' has contributions from T conserving (CPT and CP violating) and CPT conserving (CP and T violating) terms in the $I = 2$ decay amplitude ($|\Delta S| = 1$).
- ω is the ratio of the $|\Delta I| = 3/2$ to $|\Delta I| = 1/2$ decay amplitude, and is (dominantly) CP, T and CPT conserving.

Under CPT conservation, with which all experimental evidence is in agreement, $a = \delta = 0$, and $\eta_{+-} = \epsilon + \epsilon'$; $\eta_{00} = \epsilon - 2\epsilon'$. Moreover, ϕ' , the phase of ϵ' , is then predicted from measured $\pi\pi$ phase shifts to be about 45° , in good agreement with the phase of ϵ given by:

$$\phi_\varepsilon = \tan^{-1} (2 \Delta m / (\gamma_S - \gamma_L)) = 43.7^\circ \pm 0.2^\circ \quad (8)$$

Thus, the phases of η_{+-} and η_{00} should both be equal to this value.

Using K_L and K_S beams it is highly desirable to make high precision measurements of the double ratio R and of ϕ_{+-} and ϕ_{00} , the phases of η_{+-} and η_{00} respectively. These measurements are sensitive to different combinations of CP and CPT violating amplitudes, and enable rigorous consistency checks to be made. If R is found to differ significantly from unity (for example by 1%), it is still important to investigate its origin and to check whether ϕ' is close to 45° : a measurement of $\Delta\phi$ to 0.1° will enable ϕ' to be measured with a precision of 10° . Similarly, if R is consistent with unity, the check that $\Delta\phi$ is consistent with zero is important, and the measurement of ϕ_{+-} becomes particularly so in looking for CPT violation or investigating the possible cancellation of CP and CPT violating amplitudes.

A high precision measurement of the phase angle ϕ_{+-} and the difference $\Delta\phi = \phi_{+-} - \phi_{00}$ would involve a similar experimental arrangement to that considered for the measurement of ε'/ε . The phase measurement would be done in two parts. First, beams of K_S and K_L would be used in conjunction with a thin radiator to measure the phase angle $\phi = \phi_{\pi\pi} - \phi_\rho$, and secondly, semileptonic decays would be used in conjunction with a thick regenerator to measure the regeneration phase angle ϕ_ρ , together with the parameters Δm and γ_S to the necessary, increased precision.

a) $K_L \rightarrow \pi\pi$: Measurement of $\phi_{\pi\pi} - \phi_\rho$. Two identical K_L beams are used, with a thin regenerator switching from one beam to the other. The configuration is the same as described for the ε'/ε determination. Normalization is effected by comparing decay rates at time t with and without the regenerator. With time in units of τ_S , the regeneration may be written:

$$R(t) \cong [1 + |\rho/\eta|^2 e^{-t} + 2|\rho/\eta| e^{-t/2} \cos(\Delta m t - \phi)] \quad (9)$$

To measure ϕ to 0.1° requires $|\rho/\eta|$ to be fitted to about one part in 10^3 , with a similar accuracy in the knowledge of Δm and in the time (momentum) scale.

The optimum value for $|\epsilon/\eta|$ is about 1, therefore a few million $\pi^+\pi^-$ and $\pi^0\pi^0$ decays are sufficient to give a statistical accuracy of 0.1° on the measurement of $\phi = \phi_{\pi\pi} - \phi_\rho$, and $\Delta\phi = \phi_{+-} - \phi_{00}$.

b) $K_L \rightarrow \pi^\pm e^\mp \nu$: measurement of ϕ_ρ . In order to maximize the difference in decay rate to electrons and positrons a thick regenerator (2 interaction lengths corresponding to $|\rho| \approx 0.05$) is used in conjunction with two identical K_L beams.

Assuming $\Delta S = \Delta Q$ in the decay, the rates to e^+ and e^- are:

$$R(\pm)_t = (1 \pm 2\epsilon) [1 + |\rho|^2 e^{-t} \pm 2|\rho|e^{-t/2} \cos(\Delta m t - \phi_\rho)] \quad (10)$$

Hence a time dependent asymmetry may be defined

$$A(t) = \frac{R(+)-R(-)}{R(+)+R(-)} = \frac{2 \left[\epsilon + |\rho| e^{\frac{-t}{2}} \cos(\Delta m t - \phi_\rho) \right]}{1 + |\rho|^2 e^{-t}} \quad (11)$$

where terms of order $|\rho|\epsilon$ have been ignored.

To measure ϕ_ρ to 0.1° implies determining ρ to one part in 10^3 , with similar accuracy in Δm and in the time scale. It is also necessary to improve the measurement of ϵ somewhat beyond its present value of 3%. To gain the required statistical accuracy, a few hundred million K_L decays to e^+ and e^- must be identified.

It may be that the systematic errors are better controlled by using a thick radiator in each of the two K_L beams, but separated along the beam direction by about $3 \tau_s$ (corresponding to $\Delta m \approx 90^\circ$). This idea, to be used in E773, has less sensitivity to $|\rho|$ and maximizes sensitivity to ϕ_ρ .

3. SEARCHING FOR $K_L \rightarrow \pi^0 e e$

The purpose of this section is to examine the feasibility of measuring direct CP violation in the decay $K_L \rightarrow \pi^0 e e$. The current experimental upper limits on the branching ratio for this decay are at the level of 10^{-8} [11]. The Standard Model predicts that this decay should occur at a branching ratio of about 10^{-11} . Of course, there is also the possibility of discovering "new physics", should this decay be observed at a branching ratio above the Standard Model prediction.

3.1. Experimental Strategies

In principle there are several ways in which CP violation could be observed in $K_L \rightarrow \pi^0 e e$. Perhaps the best way would be to measure K_L - K_S interference as a function of proper time. The advantages of this method are first, that the presence of interference is an unambiguous signature of CP violation, and second, that one obtains information on both the magnitude and phase of the direct CP violating amplitude. Unfortunately, an interference experiment is more difficult than either a pure K_L or a pure K_S experiment, for reasons that we explain below.

One of the most difficult backgrounds to $K_L \rightarrow \pi^0 e e$ is an accidental coincidence between the decay $K_L \rightarrow \pi e \nu$, where the pion is mis-identified as an electron, and a π^0 . In a pure K_L beam, the main sources of accidental π^0 's are $K_L \rightarrow \pi^0 \pi^0 \pi^0$ and $K_L \rightarrow \pi^+ \pi^- \pi^0$. In both cases there are extra particles that can be used to veto the event. Making the veto system as hermetic as possible will be an important strategy in reducing this background. In the interference region, there are the following additional sources of π^0 's: $K_S \rightarrow \pi^0 \pi^0$, $\Lambda \rightarrow n \pi^0$, and, $\Xi^0 \rightarrow \Lambda \pi^0$. In the last two cases there will be no extra particles to veto on when, as is likely, the final state neutral baryons go down the beam hole. Also, an interference experiment can expect higher rates generally because it must be closer to the production target.

In view of the above difficulties, we are going to concentrate on the two experiment method of measuring direct CP violation. That is, one measures the branching ratios for $K_S \rightarrow \pi^0 ee$ and $K_L \rightarrow \pi^0 ee$ in separate experiments and looks for a deviation from purely indirect CP violation.

3.2. Theoretical Expectations

3.2.1. The CP violating contribution to $K_L \rightarrow \pi^0 ee$ The decay mode $K_L \rightarrow \pi^0 ee$ is CP violating in lowest order (i.e. through a single intermediate photon). As with $K_L \rightarrow \pi\pi$, $K_L \rightarrow \pi^0 ee$ is predicted to receive contributions from both indirect and direct CP violation. Unlike $K_L \rightarrow \pi\pi$, the direct contribution to $K_L \rightarrow \pi^0 ee$ is predicted to be comparable to the indirect contribution. Furthermore, the direct contribution to $K_L \rightarrow \pi^0 ee$ is predominantly a short distance phenomenon, and therefore calculable without large theoretical uncertainties.

The contribution to $K_L \rightarrow \pi^0 ee$ from indirect CP violation is given by $\Gamma(K_L \rightarrow \pi^0 ee) = |\epsilon|^2 \Gamma(K_S \rightarrow \pi^0 ee)$ where $|\epsilon| = 2.3 \times 10^{-3}$ as measured in $K^0 \rightarrow \pi\pi$. The rate for $K_S \rightarrow \pi^0 ee$ is not known. We can, however, get an order of magnitude estimate from the measured rate for $K^+ \rightarrow \pi^+ ee$. If $\Gamma(K_S \rightarrow \pi^0 ee) = \Gamma(K^+ \rightarrow \pi^+ ee)$ then $B(K_L \rightarrow \pi^0 ee) = 6 \times 10^{-12}$. The rate for $K_S \rightarrow \pi^0 ee$ has been predicted to be 0.25 or 2.5 times the rate for $K^+ \rightarrow \pi^+ ee$ ¹²⁾.

The contribution of direct CP violation to $K_L \rightarrow \pi^0 ee$ has been calculated by several theoretical groups^{13,14)}. The authors of Ref. 14 have pointed out that for large top quark mass, purely weak processes are important, and that for sufficiently heavy top are even the dominant contribution to the direct CP violation amplitude. The predicted branching ratio for $K_L \rightarrow \pi^0 ee$, including indirect CP violation is¹⁴⁾

$$B(K_L^0 \rightarrow \pi^0 ee) \approx \left[\left| 0.76 \left(e^{\frac{i\pi}{4}} - i \frac{\xi}{|\epsilon|} \right) \tilde{R} + i \left(\frac{s_2 s_3 s_\delta}{10^{-3}} \right) \tilde{C}_{7V} \right|^2 + \left| \left(\frac{s_2 s_3 s_\delta}{10^{-3}} \right) \tilde{C}_{7A} \right|^2 \right] \times 10^{-11} \quad (12)$$

The \tilde{R} term represents the contribution from indirect CP violation where $\tilde{R} = A(K_L \rightarrow \pi^0 ee)/A(K^+ \rightarrow \pi^+ ee)$. The parameter ξ is related to direct CP violation in $K_L \rightarrow \pi\pi$ ($\xi = 0$ if $|\epsilon'/\epsilon| = 0$). The \tilde{C}_{7V} and \tilde{C}_{7A} terms are the contributions from direct CP violation via effective vector and axial-vector couplings to the electron pair. The single photon contribution is contained in \tilde{C}_{7V} . The values of \tilde{C}_{7V} and \tilde{C}_{7A} depend on the mass of the top quark as shown in Table 5. The $s_2 s_3 s_8$ factor represents the product of the Kobayashi-Maskawa mixing angles.

Table 5. \tilde{C}_{7V} and \tilde{C}_{7A} as a Function of Top Quark Mass.

$m_t(\text{GeV})$	\tilde{C}_{7V}	\tilde{C}_{7A}
50	-0.32	0.10
100	-0.46	0.30
150	-0.54	0.57
200	-0.62	0.89

3.2.2. The CP conserving contribution to $K_L \rightarrow \pi^0 ee$. In addition to the CP violating contributions to $K_L \rightarrow \pi^0 ee$, there is a CP conserving contribution that proceeds through a two-photon intermediate state (i.e. $K_L \rightarrow \pi^0 \gamma\gamma \rightarrow \pi^0 ee$). Unfortunately, theory can not at the present time make a reliable prediction of the size of the CP conserving two-photon process. The problem is due to uncertainty in the relative magnitudes of the S-wave and D-wave amplitudes (also called the A and B amplitudes) for $K_L \rightarrow \pi^0 \gamma\gamma$. The conversion $\gamma\gamma \rightarrow ee$ is helicity suppressed for the S-wave, but not for the D-wave term. Only the D-wave (or B) term can make a significant contribution to $K_L \rightarrow \pi^0 ee$.

The B term is higher order in chiral perturbation theory than the A term. Although the relative magnitudes of the A and B terms are not fixed in chiral perturbation theory, dimensional analysis suggests that the B term should be small compared to the A term, in which case the CP conserving rate for $K_L \rightarrow \pi^0 ee$ would be

negligible in comparison to the CP violating rate¹⁵⁾. On the other hand, vector meson dominance models predict that the A and B terms should be approximately equal in magnitude^{16,17)}. If these models are correct, then the CP conserving contribution to $K_L \rightarrow \pi^0 ee$ could be comparable to the CP violating contributions. Ultimately, the size of the D-wave contribution to $K_L \rightarrow \pi^0 \gamma \gamma$ will have to be determined experimentally. Should it turn out that the CP conserving contribution to $K_L \rightarrow \pi^0 ee$ is significant, all is not lost. Since the CP conserving and CP violating final states have different quantum numbers, it should be possible to separate their contributions by analyzing the Dalitz plot¹⁷⁾.

3.3. Discussion of Experimental Sensitivities.

In this section we evaluate numerically the feasibility of discovering direct CP violation by the two experimental methods. We optimistically assume that the CP conserving contribution to $K_L \rightarrow \pi^0 ee$ is negligible. The branching ratio for $K_L \rightarrow \pi^0 ee$ is given by Eq. 12, which is evaluated assuming $\xi = 0$ and $s_2 s_3 s_8 = 10^{-3}$.

$$B(K_L^0 \rightarrow \pi^0 ee) \approx \left[\left| 0.76 e^{\frac{i\pi}{4}} \tilde{R} + i \tilde{C}_{7V} \right|^2 + |\tilde{C}_{7A}|^2 \right] \times 10^{-11} \quad (13)$$

$$= (0.58 \tilde{R}^2 + 1.07 \tilde{R} \tilde{C}_{7V} + \tilde{C}_{7V}^2 + \tilde{C}_{7A}^2) \times 10^{-11} \quad (14)$$

The branching ratio for $K_S \rightarrow \pi^0 ee$ is given by

$$B(K_S^0 \rightarrow \pi^0 ee) = B(K^+ \rightarrow \pi^+ ee) \frac{\tau_{K_S^0}}{\tau_{K^+}} \tilde{R}^2 \quad (15)$$

$$= 1.9 \times 10^{-9} \tilde{R}^2 \quad (16)$$

A positive result would require a non-zero value for a quantity, ΔB , which is the difference between the actual branching ratio for

$K_L \rightarrow \pi^0 ee$ and the branching ratio that would be predicted from state mixing only.

$$\Delta B = B(K_L^0 \rightarrow \pi^0 ee) - |\epsilon|^2 \frac{\tau_{K_L^0}}{\tau_{K_S^0}} B(K_S^0 \rightarrow \pi^0 ee) \quad (17)$$

$$= B(K_L^0 \rightarrow \pi^0 ee) - 0.003 B(K_S^0 \rightarrow \pi^0 ee) \quad (18)$$

Suppose that K_L and K_S experiments are performed with single event sensitivities of S_S and S_L respectively. The number of events detected in the two experiments will be

$$n_s = \frac{B(K_S^0 \rightarrow \pi^0 ee)}{S_s} \quad (19)$$

and

$$n_L = \frac{B(K_L^0 \rightarrow \pi^0 ee)}{S_L} \quad (20)$$

The size of the direct CP violation signal (Eq. 18) will be

$$\Delta B = S_L n_L - 0.003 S_s n_s \quad (21)$$

The statistical error associated with ΔB is

$$\sigma_{\Delta B} = [S_L^2 n_L + (9 \times 10^{-6}) S_s^2 n_s]^{\frac{1}{2}} \quad (22)$$

$$= [B(K_L^0 \rightarrow \pi^0 ee) S_L + (9 \times 10^{-6}) B(K_S^0 \rightarrow \pi^0 ee) S_s]^{\frac{1}{2}} \quad (23)$$

The statistical significance of the result, expressed as the number of standard deviations by which ΔB differs from zero (n_σ), is given by the ratio of Equations 18 and 23

$$n_\sigma = \frac{|B(K_L^0 \rightarrow \pi^0 ee) - 0.003B(K_S^0 \rightarrow \pi^0 ee)|}{[B(K_L^0 \rightarrow \pi^0 ee)S_L + (9 \times 10^{-6})B(K_S^0 \rightarrow \pi^0 ee)S_S]^{\frac{1}{2}}} \quad (24)$$

Equation 24 is the main result of this section. In evaluating Equation 24, we have assumed sensitivities for the K_L and K_S experiments of $S_S = 10^{-11}$ and $S_L = 10^{-13}$. These sensitivities were adopted as goals by our working group because they are necessary for a serious attack on the problem of CP violation in $K_L \rightarrow \pi^0 ee$, and because they appear to be feasible.

Figure 4 shows the variation for the predicted branching ratio for $K_L \rightarrow \pi^0 ee$ as a function of the parameter \tilde{R} and the top quark mass. Figure 5 shows the statistical significance (n_σ) as a function of \tilde{R} and the top quark mass. We see that, with the assumed sensitivities, direct CP violation could be established over the majority of the parameter space. Theoretical input on the sign of \tilde{R} would be very helpful.

3.4. Detector Requirements for $K_L \rightarrow \pi^0 e^+ e^-$

The detector requirements we describe here are based on the physics goal of achieving a 10^{-13} sensitivity for the $K_L \rightarrow \pi^0 e^+ e^-$ decay modes using the Main Injector. A generic neutral kaon apparatus is shown in Figure 1. As mentioned in previous articles¹⁾, the rates in the detector are very high, e.g. hottest wire with a pitch of 3 mm has a rate of 660 kHz. We also need a hermetic and fast detector to reject backgrounds which are discussed in detail for the Tevatron experiment E799 in Reference 18 and briefly for the Main Injector in the next section.

High Rate Chambers. For large scale ($> 1\text{m} \times 1\text{m}$) high rate chambers, several groups from existing rare decay experiments at BNL, KEK and Los Alamos have demonstrated what is presently achievable. The 1 mm pitch PWC with CF_4 + isobutane gas used in

the Los Alamos MEGA experiment could withstand up to 10 MHz/wire.

High Rate Photon Veto Counters. As was discussed in Section 2.2.3, the best candidate in terms of performance per price seems to be the Pb-scintillation fiber calorimeter ¹⁰⁾.

Transition Radiation Detector. The TRD design requirements of speed and minimal integrated radiation length can be simultaneously met with a fine sampling system first suggested by Dolgoshein¹⁹⁾. A fine sampling system makes optimal use of the radiator material, which dominates the total radiation length of the TRD system. Existing TRD systems²⁰⁾ which provide a pion rejection of $\times 100$ at high electron efficiency typically require 5-8% of a radiation length to do so. A fine sampling system can deliver the same pion rejection with only 2-3% (see below) of a radiation length. In addition, an optimal fine sampling system has narrow xenon gas gaps, which allow faster charge collection times. Charge collection times in conventional systems are between 300 ns and 2000 ns, which is far too long for the expected rate. Such a fine sampling system may be realized in practice by taking advantage of the now mature straw tube technology. The model detector that we studied had the following properties: each of the two TRD systems, (up-stream and down-stream of the analysis magnet), is built from 9000 4 mm diameter mylar/conductive-polycarbonate tubes with 30 micron walls spanning the 3 m gap aperture of the chamber. The tubes are arranged in 10 planes, with polypropylene fiber radiator material upstream of every detector plane. The tubes in each plane are staggered with a 3.3 mm pitch, and each plane is staggered by half a cell with respect to adjacent planes.

This system should provide:

1. A π/e rejection of better than $\times 100$ at high electron efficiency (90%) for particle momenta between 2 and 30 GeV/c.
2. Charge collection times of 30-50 ns for the 2 mm drift through fast xenon mixtures ²¹⁾ such as 80/10/10% Xe/CF₄/C₂H₂.

At a maximal charged particle rate of 660 kHz this implies a maximal occupancy of a few percent.

3. The system that we simulated had a relatively simple readout: if greater than 4 of the 10 tubes traversed had signal over threshold (4 keV), then the track was tagged as an electron. This simple criteria provided a π/e rejection always over $\times 100$ at an electron efficiency of 90%.

4. The total amount of material length including radiator, tubes and gas was between 2.2% and 2.5% of a radiation length.

5. No significant variation of π/e rejection was seen vs. track position across the aperture of the chamber. Hence the tube staggering solved this problem well.

3.5. Backgrounds to $K_L \rightarrow \pi^0 e^+ e^-$

We estimated the major backgrounds expected for $K_L \rightarrow \pi^0 e^+ e^-$ decay at the Main Injector. These are $K_L \rightarrow e^+ e^- \gamma + \gamma_{acc}$, $K_L \rightarrow \pi e \nu \gamma + \gamma_{acc}$, and $K_L \rightarrow \pi e \nu + 2\gamma_{acc}$, where pions are mis-identified as electrons, and γ_{acc} is an accidental photon hitting the electromagnetic calorimeter. The background level is calculated by :

$$BGL = BR \times (\pi/e)^{\# \pi} \times R_\gamma \times \Delta t \times \frac{Acc(bkg)}{Acc(signal)} \quad (25)$$

where BR is the branching ratio of the decay involved, (π/e) is the pion rejection factor, $\# \pi$ is the number of pions in the decay, R_γ is the accidental photon rate, Δt is the time resolution of the detector, $Acc(bkg)$ and $Acc(signal)$ are the acceptance of the background and signal events.

We assumed the standard detector for the Main Injector¹⁾, with an electromagnetic calorimeter resolution of $3\%/\sqrt{E}$, and a momentum resolution of 1%. The selection criteria were :

- a) 4 clusters with >1 GeV each in the calorimeter.
- b) no particles outside the calorimeter (perfect photon vetos)
- c) $|m_{\gamma\gamma} - m_{\pi^0}| < 5 \text{ MeV}/c^2$ (2σ)
- d) $|m_{ee\gamma\gamma} - m_K| < 7.5 \text{ MeV}/c^2$ (2σ)

- e) $P_t^2 < 45 \text{ (MeV/c)}^2$ (4σ) where P_t^2 is the transverse momentum square of $e\bar{e}\gamma\gamma$ system with respect to the kaon
- f) $m_{e\bar{e}} > 150 \text{ MeV/c}^2$ to reject π^0 Dalitz decay
- g) $m_{e\bar{e}\gamma} < 480 \text{ MeV/c}^2$ (for the mass combination closer to m_K to suppress kaon Dalitz decay
- h) $E_K > 15 \text{ GeV}$.

We generated kaons between 5 GeV and 50 GeV, and decays between 25 m and 45 m from the target, for both signal and background events. Since we generated kaons below 15 GeV, $\text{Acc}(\text{signal})$ is 3.3%, whereas it is actually 13% if kaons only above 15 GeV are considered.

We considered accidental photons from $K_L \rightarrow 3\pi^0$ which decayed between the target and the calorimeter with $E_K = 1 \text{ GeV}$ to 50 GeV and normalized to the standard instantaneous kaon decay rate of 33 MHz ($15 \text{ GeV} < E < 50 \text{ GeV}$, $25\text{m} < z < 45\text{m}$). The rate of having one (two) or more photons $> 1 \text{ GeV}$ in the calorimeter without hitting the photon veto system downstream of the beam dump was 21 MHz (14 MHz). Most of these decays occurred at the last part of the beam dump or near the electromagnetic calorimeter, where all the photons which did not hit the calorimeter either hit the beam dump or escaped down the beam hole.

The background acceptances were found by overlaying a kaon decay event with an accidental photon event. The $\text{Acc}(\text{bkg})$'s were: $A(K_L \rightarrow e^+e^-\gamma + \gamma_{\text{acc}}) = 7.7 \times 10^{-10}$, $A(K_L \rightarrow \pi e \nu \gamma + \gamma_{\text{acc}}) < 1.4 \times 10^{-6}$ (90%CL), and $A(K_L \rightarrow \pi e \nu + 2\gamma_{\text{acc}}) = 1.4 \times 10^{-5}$. The first acceptance is small because of the $m_{e\bar{e}\gamma}$ cut. The background levels are summarized in Table 6 using; $(\pi/e) = 10^{-5}$, and $\Delta t = 1\text{ns}$.

Table 6. Backgrounds to $K_L \rightarrow \pi^0 e^+ e^-$

Background	BR	# π	R_γ	Acc(bkg)	BGL
$K_L \rightarrow e^+ e^- \gamma + \gamma_{acc}$	1.7×10^{-5}	0	21MHz	7.7×10^{-10}	8.3×10^{-15}
$K_L \rightarrow \pi e \nu \gamma + \gamma_{acc}$	1.9×10^{-2}	1	21MHz	$< 1.4 \times 10^{-6}$	$< 1.7 \times 10^{-13}$
$K_L \rightarrow \pi e \nu + 2\gamma_{acc}$	0.39	1	14MHz	1.4×10^{-5}	2.3×10^{-11}

The largest background is K_{e3} with two accidental photons, and even if we put photon veto counters at the end of the beam dump and veto $3\pi^0$ decays in the beam dump, the background level only goes down to 9×10^{-12} . In addition, if we veto on accidental photons down the beam hole (this could be done by having several layers of photon vetoes with a beam hole at the downstream of the calorimeter), we are left with one event where 4 photons from $3\pi^0$ decay were going backward in the lab. This corresponds to a background level of 1×10^{-12} , which is still 10 times larger than the sensitivity we would like to achieve.

The conclusion of the background study is therefore:

1. We need a photon veto counter at the end of the beam dump to veto $3\pi^0$ decays.
2. We need a photon veto downstream of the calorimeter beam hole to veto $3\pi^0$ decays near the calorimeter.
3. The product of the π/e rejection factor and the time resolution of the detector should be smaller than 10^{-6} ns.

4. SEARCHING FOR $K_L \rightarrow \mu e$

4.1. Introduction

Some of the attempts to replace the Standard Model with more satisfactory theories (such as Supersymmetry, Technicolor, GUTs or E6 models) result in predictions that lepton flavor (separate lepton number) is not absolutely conserved. A new generation of experiments is underway to study decays in which lepton flavor conservation might be violated, such as $K_L \rightarrow \mu^\pm e^\mp$,

$K^+ \rightarrow \pi^+ \mu^+ e^-$, $\mu \rightarrow e \gamma$, $\mu \rightarrow e e e$, and $\mu^- A \rightarrow e^- A$. Since the form of a lepton number violating interaction is unknown, it is useful to probe all of these decays, and perhaps decays of B and D mesons, to whatever level is technically feasible. However, here we concentrate on the decay $K_L \rightarrow \mu^\pm e^\mp$.

The three most recent experiments on this process have been E780 at BNL²²⁾, E791 at BNL²³⁾, and E137 at KEK²⁴⁾, which currently report (90% C.L.) upper limits on the branching fraction of 1.9×10^{-9} , 2.2×10^{-10} , and 4.3×10^{-10} respectively. While E780 is complete, the other two experiments are in the process of collecting larger samples and a combined sensitivity of about 2×10^{-11} is likely (by sensitivity we mean the branching fraction which would produce one observed event). Any new experiment should aim at a sensitivity of 10^{-13} . There are several places which might offer a suitable beam: the BNL AGS with the Booster (and the planned Stretcher), the Fermilab Main Injector, and the TRIUMF KAON facility. While the Main Injector is not planned to have as intense a beam as the other facilities, its higher energy boosts the kaon spectrum so that more particles are in the useful momentum range.

Attempting to reach a sensitivity of 10^{-13} makes many demands and it is clear that improvements in technology are needed. A detailed consideration of many aspects of a Main Injector experiment on $K_L \rightarrow \mu^\pm e^\mp$ is given by Heinson et al. in the report of the 1989 Workshop on Physics at the Main Injector²⁵⁾. Here we review some general points.

4.2. Sensitivity

This is determined by the product of several basic factors. We list them below, using typical values for a beam at the Main Injector (production energy of 120 GeV, solid angle of $36 \mu\text{str}$, 3×10^{13} protons on target).

- K_L decays in 20 m decay volume: $2.5 \times 10^{11}/\text{hr}$
- Acceptance: 10% of $K_L \rightarrow \mu^\pm e^\mp$ decays in the decay volume

- Data-taking time: 4000 hours
- Experimental efficiency: 0.25

This would result in the observation of 2.5×10^{13} decays, so that an upper limit of 10^{-13} is possible, if background and rate-related problems can be solved.

4.3. Rates

Even if the beam quality is excellent so that most of the rate in the detectors comes from K_L decays, rates will be high enough to require new technologies. An apparatus with large acceptance for $K_L \rightarrow \mu e$ will also have a large (e.g. 60%) acceptance for single charged particles from K_L decays. At the beam intensity envisaged, K_L decays alone will give rates of 50 ~ 100 MHz in the detectors. Also, the rate of accidental coincidences of a muon from $K_L \rightarrow \pi \mu \nu$ and an electron from $K_L \rightarrow \pi e \nu$ will be of the order of 1 MHz, given a resolving time of 10 ns. Additional μe events will come from $K_L \rightarrow \pi e \nu$, followed by π decay in flight, at a rate of 250 kHz. This presents challenges to detector, trigger, and pattern recognition technologies. All these problems can be ameliorated by a Stretcher ring to provide up to 80% duty factor. It is assumed that the beam is de-bunched before extraction from the Main Injector.

4.4 Backgrounds

4.4.1. $K_L \rightarrow \pi e \nu$ followed by $\pi \rightarrow \mu \nu$ decay in flight. This can be minimized by reducing the length of the decay volume, and rejected by careful reconstruction of the event. Reducing the path length available for π decay also reduces, in the conventional approach, the decay volume for kaon decay so this is not a useful approach. (In a proposed solenoidal geometry²⁶), this conflict does not occur.) In this sequence of decays, the minimum energy of the neutrinos in the kaon CM is 8.4 MeV/c², so the invariant mass of the μe has a maximum value of $m_K - 8.4 \text{ MeV}/c^2$.

Experiments thus rely on reconstructing the invariant mass of the μe pair to reject this background. The invariant mass of the pair is $m = p_1 p_2 \theta^2$, where p_1, p_2 are the measured momenta and θ is the opening angle. If we consider an apparatus consisting of position-measuring devices (e.g. drift chambers), precision σ_x , separated by space length l , and a ratio of thickness to radiation length of L/L_{rad} followed by a dipole giving a transverse impulse of Δp , the mass resolution at the kaon mass is given by:

$$\left(\frac{\sigma_m}{m}\right)^2 \approx \frac{\sigma_x^2 p_K^2}{l^2 \Delta p^2} \left[\frac{5}{4} + \frac{1}{4} \frac{\Delta p^2}{m_K^2} \right] + \frac{p_{ms}^2}{\Delta p^2} \frac{L}{L_{\text{rad}}} \left[2 + \frac{1}{2} \frac{\Delta p^2}{m_K^2} \right] \quad (26)$$

where $p_{ms} = 14 \text{ MeV/c}$. For other geometries the numerical factors will change, but remain of order $1/4 \sim 2$. Thus the mass resolution has a term which depends on p_K and σ_x , and another which depends on the ratio of multiple scattering to magnetic field. Values for E791 are $\sigma_x = 0.1 \text{ mm}$, $l = 1.5 \text{ m}$, $p_K = 4 \sim 16 \text{ GeV/c}$, $\Delta p = 0.3 \text{ GeV/c}$, and $L/L_{\text{rad}} = 10^{-3}$. With those values, the average mass resolution is 1.4 MeV/c^2 , and the two terms in the above expression are equal at 8 GeV/c .

With this resolution, a Monte Carlo simulation indicates a background at or below the 10^{-13} level; however, the E791 experience does not follow the simulation²⁵⁾ and has more background at high mass by a factor of up to 10. This may be due to inaccuracies in the magnetic field or non-gaussian shapes for resolution functions. Presumably, these problems can be resolved in a future experiment by technical improvements. It should be noted that a dependable way of improving the shape of a resolution function is to make multiple measurements. Typically, decreasing σ_x in this way increases L/L_{rad} , so this needs careful study.

4.4.2. Accidental coincidences of $K_L \rightarrow \pi e \nu$ and $K_L \rightarrow \pi \mu \nu$. This is also dealt with by reconstructing the event, making sure that the two tracks come from a common vertex, have low transverse

momentum relative to the kaon momentum, and the correct invariant mass. Good timing resolution in the trigger and offline is also important. De-bunching of the Main Injector extracted beam is extremely important. The proposal for E791 used a time resolution of 2 ns and determined that this would cause a background of 8 events at a sensitivity of 10^{-12} and a beam of 10^{13} protons/spill. This background goes as the square of the rate of K_L decays, which are higher at the proposed Main Injector K_L beams. Rejection is difficult; one method is to reject events with an additional track pointing to the 'vertex,' or indeed any additional track.

4.4.3. Double mis-identification. This refers to $K_L \rightarrow \pi e \nu$ decay, with double mis-identification of the particles (π as e , e as μ). If the ' e ' has a higher momentum than the ' μ ', this can result in a reconstructed mass at the kaon mass. This is reduced by good particle identification and by a cut on $(p_e - p_\mu) / (p_e + p_\mu)$. Retaining events with this parameter < 0.25 will reject almost all double mis-identified events with mass greater than $0.490 \text{ GeV}/c^2$, while retaining 90% of μe events. Without this cut, the particle identification must reduce the likelihood of double mis-identification to 10^{-9} or better.

4.4.4. Events from beam-gas interactions. The experience of E791 suggests that events causing a μe trigger are multiple-pion production events. They can reconstruct to any invariant mass. Maintaining an excellent vacuum in the decay volume (0.1 mTorr), and having good particle identification will reduce these events adequately.

4.5. Geometry and Event Selection

The conventional geometry is a two-arm spectrometer, with two magnets in each arm to measure the momentum twice, discriminating against decays in flight and improving the measurement. In BNL E791 the bends are in opposite directions

and of magnitude $\Delta p = 0.3 \text{ GeV/c}$, so that both signs of particles are accepted in either arm. In KEK E137 the bends are in the same direction with a total $\Delta p = 0.22 \text{ GeV/c}$. This allows a trigger based on the particles being parallel to the beam, but means that only one sign of particle is accepted in each side, cutting the acceptance in half. The advantage of this trigger is that it discriminates well against $K_L \rightarrow \pi e \nu$ events, by a factor of 15 or more. In BNL E791 this discrimination is done in an on-line processor (Level 3), although an existing hardware processor (Level 2) can give a factor of three reduction. The advantage of the E791 arrangement is better momentum resolution, useful for higher kaon momentum.

Another arrangement might be an asymmetrical one, with opposite bends of 0.44 GeV/c and 0.22 GeV/c , to allow a parallel to beam trigger with its consequent reduction of computing requirements.

4.6. Particle Identification

Particle identification is usually done twice, with one method used in the trigger. Electrons can be identified with gas Cerenkov counters, TRDs and total-absorption shower detectors. Muons are identified by having a long range and small scattering in matter; detailed correspondence between the range and momentum can also be used. In the case of both BNL E791 and KEK E173, Cerenkov counters and lead-glass shower counters were used to identify electrons, and a minimum range requirement was used for muons (this requirement was not stringent enough to reject pion decays in flight). Cerenkov counters give a fast signal, but the length necessary for good efficiency goes as the square of the desired pion threshold momentum.

For example, for a pion threshold of 8 GeV/c , 3 m of gas of the appropriate refractive index is needed. Assuming that it is satisfactory to reject all particles above 10 GeV/c at the Main Injector, a length of 4.7 m would be needed to have this as the pion threshold. A fast TRD that could be used in a short-resolving-time

trigger would be a compact alternative and would be useful in on- or off-line processing.

For the shower counters, lead glass is not acceptable because of radiation damage; other materials must be used (see section 2.2.3).

There are two particle identification problems: rejecting pions masquerading as muons to reduce background from $K_L \rightarrow \pi e \nu$, and rejecting pions imitating electrons and electrons imitating muons to reduce the double mis-identification background. In the first case, pion decays in flight are the main source of mis-identification; about 5% decay in flight in E791. Matching the range to the momentum to about 10% can reduce this by a factor of five.

In the second case, KEK E137 has the following particle identification figures: for a pion imitating an electron, about 1% in two detectors (gas Cerenkov counters and lead glass counters); and for an electron imitating a muon in the electron detectors, about 1%, and in the muon detector about 10^{-3} . So the overall double mis-identification probability is 10^{-9} . At the Main Injector, accidentals reduce this rejection somewhat, making a TRD necessary.

4.7. Computing Power and Pattern Recognition

Estimated computing needs for online and offline processing are in range of 1,000 MIPS; this will likely be available at the time an experiment is mounted.

In BNL E791, pattern recognition was a significant problem, since single rates in the drift chambers were high and the number of planes used was close to the minimum needed for reconstruction. For a Main Injector experiment, pattern recognition will need to be improved by redundancy of position measurement while minimizing the increased multiple scattering. Increased on-line processing power will also be needed to incorporate more detailed algorithms than were used in E791.

4.8. Conclusion on $K_L \rightarrow \mu \pm e \mp$

A $K_L \rightarrow \mu \pm e \mp$ experiment at the Main Injector is worth further study. The Main Injector has advantages over lower energy machines, particularly because more of the kaons produced are in a useful momentum range. Aspects that need study are control of the tails of the mass resolution, particle identification and improved pattern recognition in a high rate environment, if a sensitivity of 10^{-13} is to be reached.

5. FUTURE OPTIONS

During this Workshop a proposal²⁷⁾ was made to add a stretcher ring to the Main Injector. This would be a second synchrotron ring located in the Main Injector tunnel operating DC at 120 GeV. The advantage of this scheme is nearly 100% slow spill duty factor versus 30% duty factor in the standard upgrade plan. Also, by removing the 1 second slow spill period from the Main Injector cycle this increases the number of protons available by 50%. There was also some discussion of a prebooster ring which could increase the available flux by a factor of 8.

Improved duty cycle is a very valuable feature for all experiments considered. The ϵ'/ϵ and $K_L \rightarrow \mu e$ experiments could make excellent use of 10^{14} protons per second. The $K_L \rightarrow \pi^0 e e$ experiment (accidental limited) could go to a smaller beam hole (improved acceptance). Improvements in flux by going to energies lower than 120 GeV are not desirable.¹⁾

6. CONCLUSIONS

We have considered a variety of physics, beam and detector issues for the next generation of rare kaon decay studies and we believe that substantial progress was made on a number of issues. There is still a great deal of work to be done before viable proposals can be generated; nevertheless, we find the outlook for incisive experiments in this domain at Fermilab to be superb.

There is a great deal of interest in the community for such experiments which address fundamental issues in our field. Given the proper level of support from the funding agencies and from the Laboratory, an excellent program could be carried out.

The outlook can be summarized in the following "conclusions" from our working group:

1. E731 should determine ϵ'/ϵ with a precision of 7×10^{-4} from the analysis of its full data set. If the result is still consistent with zero, then an upgraded Tevatron experiment could reach a precision of about 3×10^{-4} .

2. It appears that the Main Injector would allow an ϵ'/ϵ determination at the level of about 0.6×10^{-4} . Very clean, well-collimated beams could be constructed, thereby significantly reducing systematic uncertainty.

3. The CPT violating parameter $\phi_{00} - \phi_{+-}$ will be determined to a precision of about 0.5° in E773. At the Main Injector, an experiment with a precision of 0.1° could be carried out. In addition, ϕ_{+-} itself can be measured to similar precision; this is also an important CPT test.

4. The mode $K_L \rightarrow \pi^0 e^+ e^-$ could be seen in E799 if its branching ratio is larger than about 10^{-11} . For studies of the possible direct CP violating component of this decay, an experiment at the level of 10^{-12} or 10^{-13} will be required if found as predicted by the Standard Model. It is necessary to search for $K_S \rightarrow \pi^0 e^+ e^-$ at the 10^{-11} level, and this could be carried out at the Tevatron. In addition, the branching ratio for $K_L \rightarrow \pi^0 \gamma \gamma$ needs to be measured and this should be done in E799. It is desirable to isolate the direct CP violating effect without doing an interference experiment because of the very high level of accidental photons in the detector when it is situated close to the production target. Even in the K_L configuration, a great deal of attention needs to be paid to the issue of accidentals.

5. BNL and KEK should be able to determine the possible $K_L \rightarrow \mu e$ branching ratio with a sensitivity of 10^{-11} . An extension of this sensitivity by a factor of 100 appears possible at the Main Injector.

6. Candidates for the electromagnetic calorimeter for such rare decay experiments were considered and their response simulated with the program EGG. BaF_2 and PbF_2 appear to be the best choices.

7. A stretcher ring, which would improve the duty cycle for the beam extracted from the Main Injector by a factor of about 3, would be desirable for all of the considered experiments because of the instantaneous rate in the detector.

8. A prebooster ring that would increase the available flux by another factor of 8 would allow much more flexibility; more experiments might run simultaneously and cleaner beams could be built. Experiments on the 2π and μe modes, which may not be intensity-limited, could be improved to take advantage of the additional flux.

REFERENCES

1. Winstein, B., Bock, G. and Coleman, R., EFI 89-01 preprint January 1989.
2. Kubota, S. et al., Nucl. Instr. and Meth. A268, 275-277 (1988).
3. Woody, C.L., private communication.
4. Laval, M. et al., Nucl. Instr. and Meth. A206, 169.(1983).
Schotanus, P. et al., Nucl. Instr. and Meth. A259, 586 (1987).
5. Woody, C.L. and Anderson, D.F., Nucl. Instr. and Meth. A265, 291 (1988) and references therein.
6. Kobayashi, H., et al., Nucl. Instr. and Meth. A270, 106 (1988).
7. Schotanus, P. et al., Nucl. Instr. and Meth. A281, 162 (1989).
8. Caffrey, A.J. et al., IEEE Trans NS 33, 230 (1986).
9. Anderson, D.F. et al., FERMILAB-Pub-89/189, to be published.
10. Hertzog, D.W. et al., Print-89-0216 (U. Illinois/Urbana), November 1988.

11. Barr, G.D. et al., Phys. Lett. B214, 303 (1988).
Gibbons, L.K. et al., Phys. Rev. Lett. 61, 2661 (1988).
12. Ecker, G., Pich, A. and de Rafael, E., Nucl. Phys. B291, 692 (1987).
13. Flynn, J. and Randall, L., preprint UCB-PTH-88-29 (November 1988).
Eeg, J.O. and Picek, I., Phys. Lett. B214, 651 (1988).
14. Dib, C.O., Dunietz, I., and Gilman, F. J., Phys. Rev. D39, 2639 (1989).
15. Ecker, G., Pich, A. and de Rafael, E., Nucl. Phys. B303, 665 (1988).
16. Morozumi, T. and Iwaskaki, H., preprint KEK-TH-206 (April 1988).
Flynn, J. and Randall, L., Phys. Lett. B216, 221 (1989).
Sehgal, L.M., preprint PITHA 89/16 (June 1989).
17. Sehgal, L.M., Phys. Rev. D38, 808 (1988).
18. Fermilab E799 Proposal.
19. Dolgoshein, B., "Transition Radiation Detectors and Particle Identification", NIM A252, 137 (1986).
20. ZEUS, VENUS, NA31.
21. Christophorou, G. et al., "Xe Containing Fast Gas Mixtures for Gas Filled Detectors", NIM 171, 491 (1980).
22. Jastrzembski, E. et al., Phys. Rev. Lett. 61, 2300 (1988).
23. Mathiazhagan, C. et al., preprint August 1989, submitted to PRL.
24. Inagaki, T. et al., Phys. Rev. D40, 1712 (1989).
25. Heinson, A., Imlay, S., Molzon, W., Urheim, J. and McFarlane, K., Workshop on Physics at the Main Injector, Fermilab, 16-18 May, 1989.
26. Wojcicki, S., private communication (E791 memo KL 209).
27. Pruss, S. and Ruggiero, A.G., these proceedings.

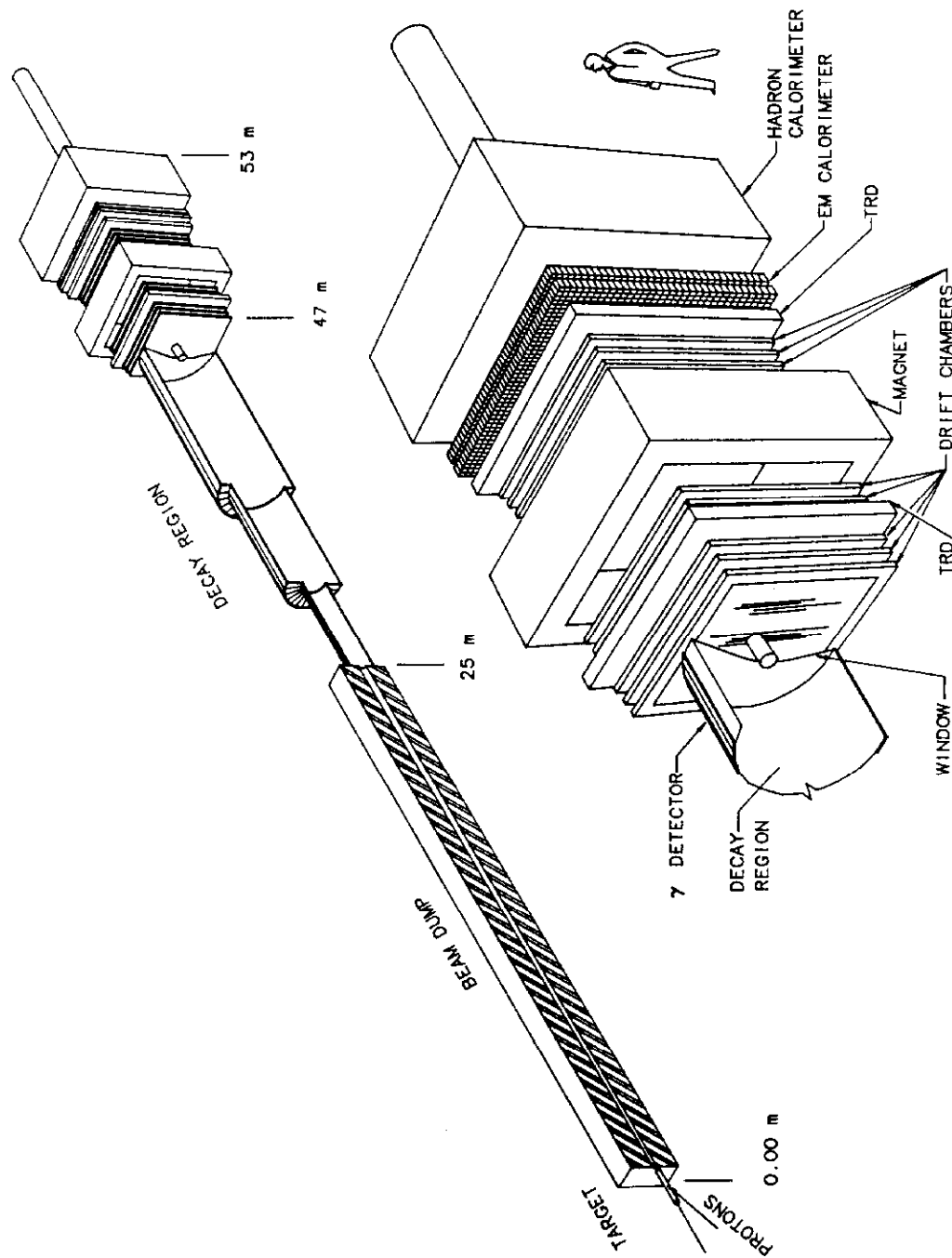


Figure 1. Model Kaon Facility at the Main Injector

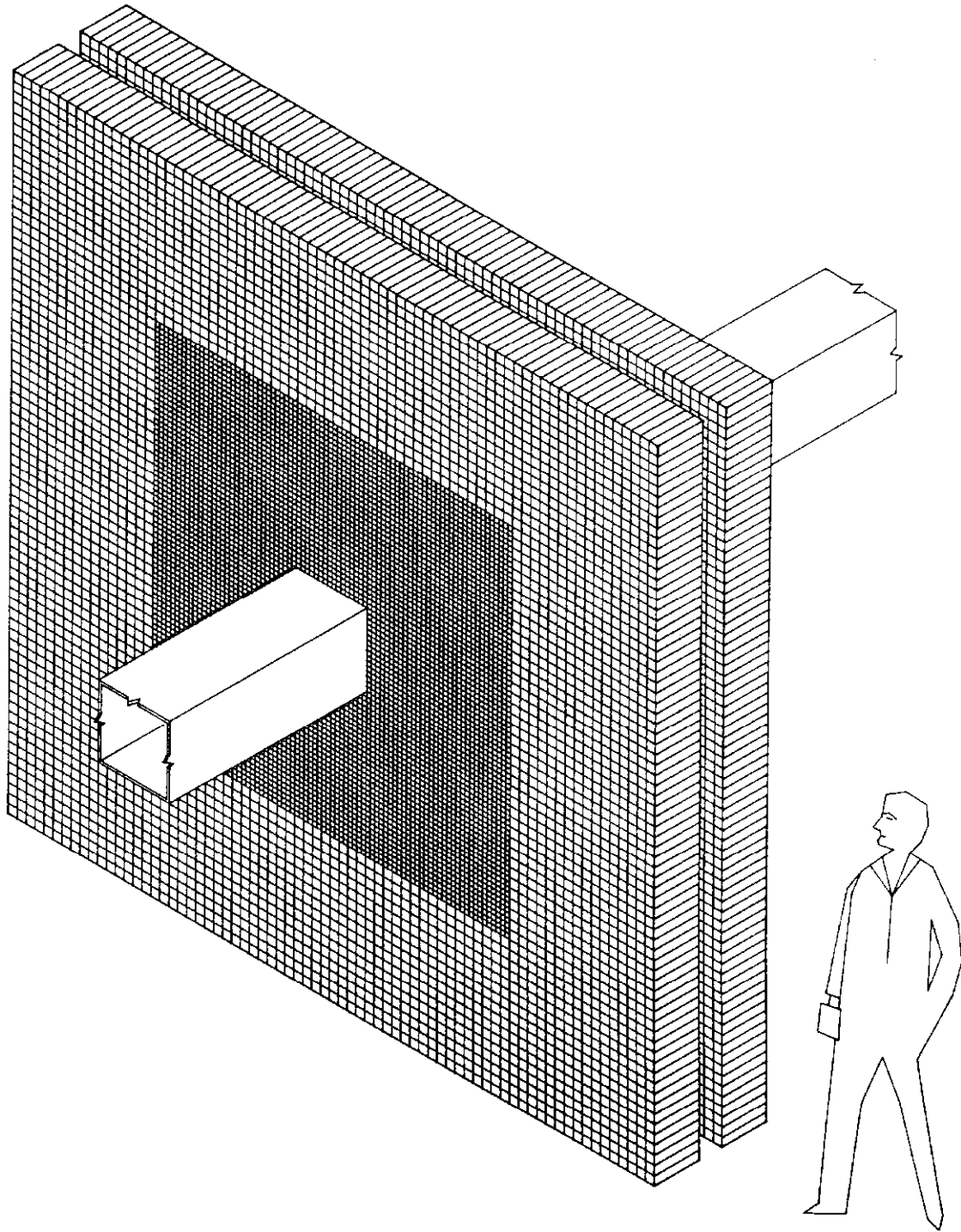


Figure 2. BaF₂ Calorimeter

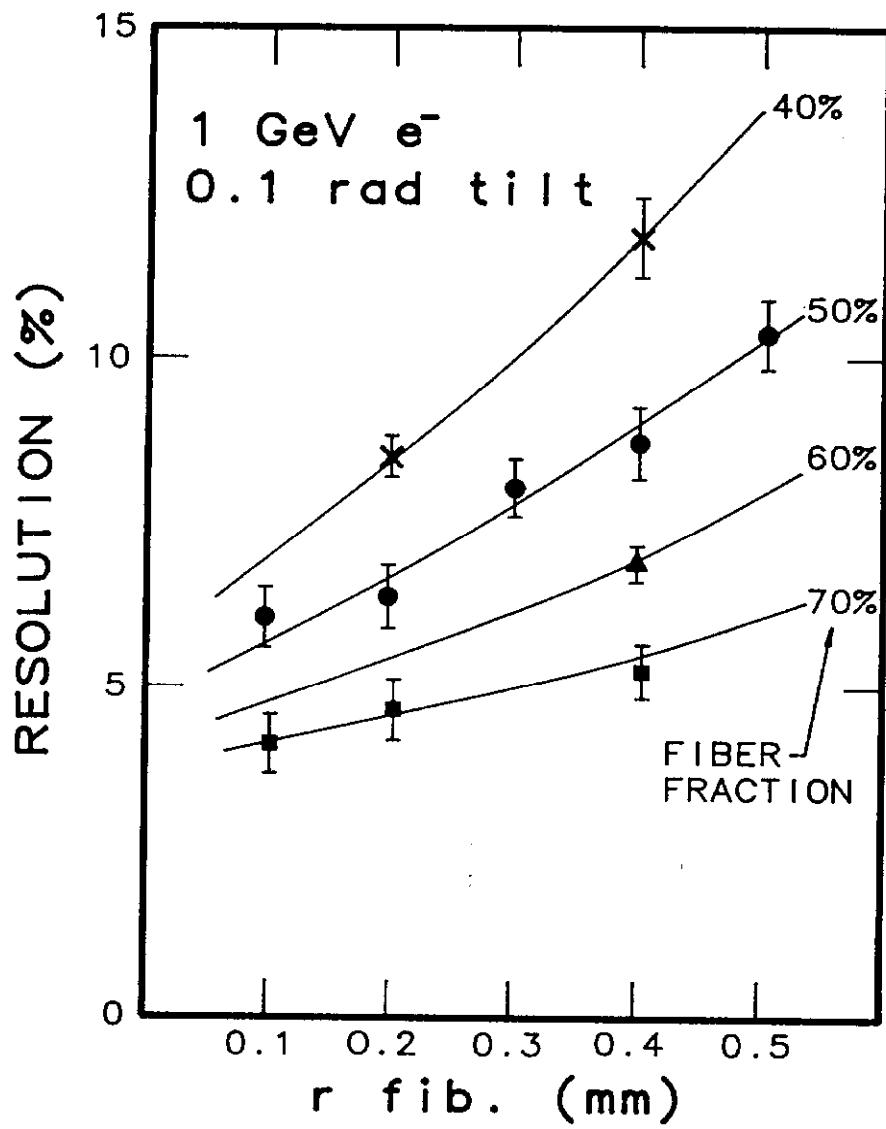


Figure 3. EGS4 Study of Lead-Scintillating
Fiber Electromagnetic Calorimeter

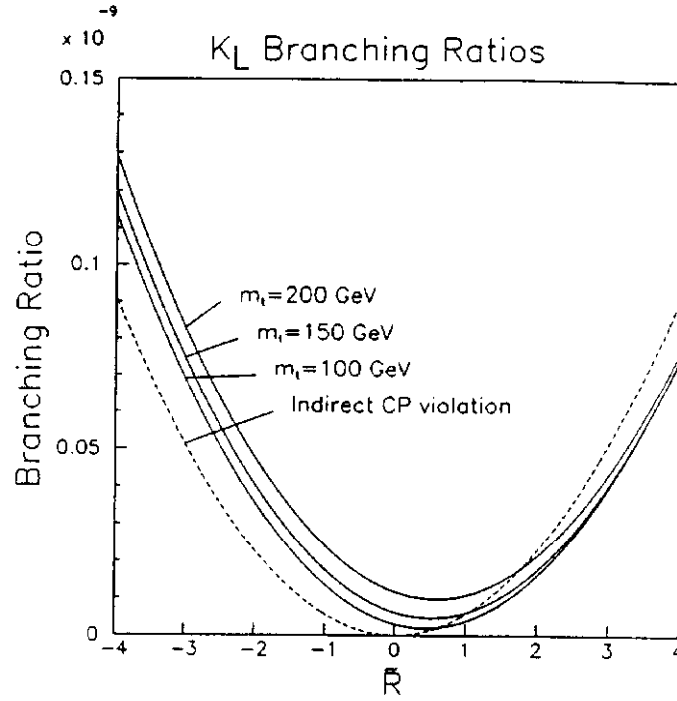


Figure 4. Branching Ratio Predictions for $K_L \rightarrow \pi^0 e e$

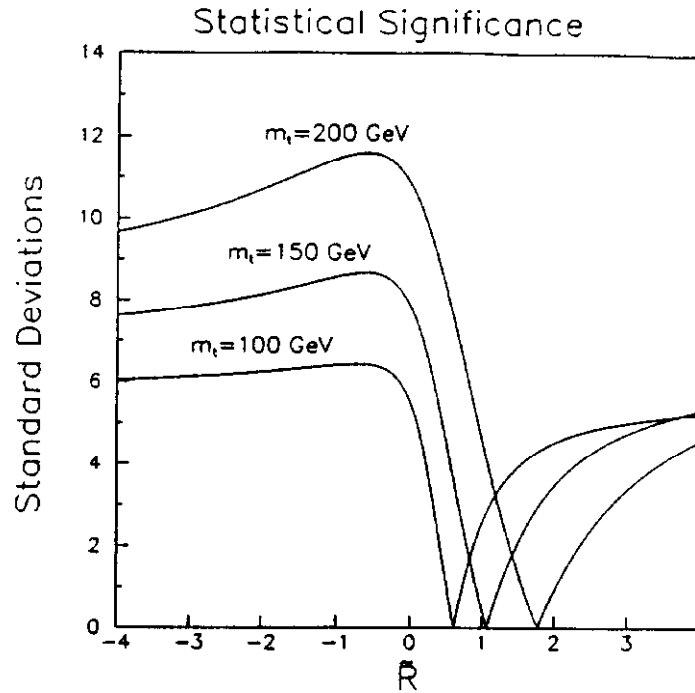


Figure 5. Statistical Significance vs \tilde{R} of Direct CP Violation in $K_L \rightarrow \pi^0 e^+ e^-$ with K_L (K_S) Sensitivity of 10^{-13} (10^{-11})